Applied Chemical Engineering (2026) Volume 9 Issue 2 ISSN: 2578-2010 (O)
doi: 10.59429/ace.v9i2.5924

ORIGINAL RESEARCH ARTICLE

Impact of abrasive material, spraying pressure, and nozzle angle on roughness of ASTM A36 steel in sandblasting processes

Riky Stepanus Situmorang[1,2,*], Novin Haritsyah[1,2], James Haryanto[1,2], Hendrik Voice Sihombing[1]

[1] *Department of Mechanical Engineering, Universitas Sumatera Utara, Medan, 20155, Indonesia*

[2] *Material Failure Analysis at Tropical Area Research Centre (MAFATA-RC), Universitas Sumatera Utara, Medan, 20155, Indonesia*

***Corresponding author:** Riky Stepanus Situmorang, rikystepanus@usu.ac.id

ABSTRACT

Sandblasting is a surface treatment process in which abrasive particles are propelled at high speed toward a material's surface to remove contaminants such as dust, paint, rust, and oil, producing a clean, rough texture. This study investigates the influence of spraying pressure, abrasive media type, and nozzle angle on the surface roughness of ASTM A36 steel. The experiment compared sandblasting results using aluminium oxide grit 60 and silica grit 60 at pressures of 5 bar and 7 bar, with firing angles of 45° and 90°. Surface roughness was measured using a roughness tester, and surface morphology was analyzed through scanning electron microscopy (SEM). The highest average roughness (Ra) for aluminium oxide was 3.819 µm at a 90° angle and 7 bar pressure, while the lowest was 2.593 µm at 45° and 5 bar. For silica abrasives, the maximum Ra was 3.651 µm under 90°–7 bar conditions, and the minimum was 2.650 µm at 45°–5 bar. These results confirm that higher pressure and perpendicular firing angles generally produce rougher surfaces due to greater abrasive energy transfer. Overall, the findings indicate that spraying pressure, firing angle, and abrasive media type significantly affect surface roughness, providing valuable insights for optimizing sandblasting parameters in industrial surface preparation.

Keywords: sandblasting; abrasive media; spraying pressure; surface roughness

ARTICLE INFO

Received: 27 February 2026
Accepted: 28 April 2026
Available online: 8 June 2026

1. Introduction

Innovation in manufacturing is essential to meet evolving industrial demands and enhance product performance. One critical stage in production is surface cleaning, where contaminants such as rust, scale, and debris are removed to prepare materials for subsequent processes[1,2]. Among various surface treatment techniques, sandblasting has become a preferred method due to its high efficiency, cost-effectiveness, and ability to produce consistent surface textures across different materials.

Sandblasting, originally developed for use in oil and gas, industrial, and fabrication sectors, involves propelling abrasive particles at high velocity toward a surface to remove unwanted layers from metals or alloys[3]. Beyond cleaning, this process also alters the material's surface roughness, which directly affects coating adhesion, fatigue resistance, and corrosion protection[2,4]. The degree of surface modification is influenced by several parameters, including nozzle angle, compressor pressure, firing distance, and abrasive particle characteristics[5–7]. For instance, steeper angles and higher pressures typically generate rougher surfaces, while variations in abrasive type can significantly change the surface morphology and energy absorption characteristics. Although numerous studies have examined the effects of individual sandblasting parameters, there remains limited experimental comparison that simultaneously evaluates the combined influence of abrasive media type, spraying pressure, and firing angle on surface roughness.

Therefore, this study aims to investigate the combined effects of abrasive media type, spraying pressure, and firing angle on the surface roughness of ASTM A36 steel during sandblasting, providing insights to optimize parameters for improved coating performance and surface preparation efficiency.

2. Materials and methods

This research based on **Figure 1** investigates how variations in sandblasting pressure and the type of abrasive medium influence the surface characteristics of ASTM A36 steel. Following specimen preparation, two abrasives—silica sand and aluminium oxide—were tested at different blasting pressure levels and nozzle angles. Following treatment, the resulting surfaces are assessed through quantitative roughness measurements and microstructural observation using a scanning electron microscope (SEM). The collected data are then interpreted to establish how variations in these process parameters influence both surface texture and morphological features.

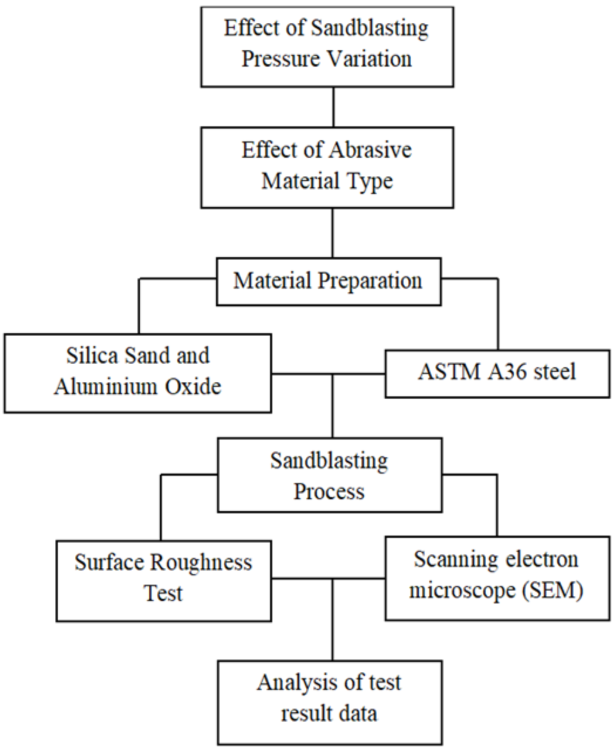

Figure 1. Conceptual Framework.

2.1. Materials

The substrate used in this study was ASTM A36 steel. Specimens were prepared from plate stock and cut to identical dimensions, then deburred, degreased with a neutral detergent, rinsed with distilled water, cleaned with alcohol, and dried prior to any treatment to ensure a uniform starting condition. The composition of ASTM A36 is shown in **Table 1**.

Table 1. ASTM A36 Composition.

Element	Content (%)
C	0.25-0.29
Cu	0.20
Fe	98.0
Mn	1.03
P	0.04
Si	0.28
S	0.05

Two abrasive types were employed: silica sand and aluminium oxide with a nominal 60-grit size shown in **Figure 2**. These abrasives were selected because they are commonly used in industrial surface preparation and represent different abrasive characteristics. Silica abrasive is a mineral-based abrasive generally used for surface cleaning, rust removal, and moderate surface preparation, although its use requires careful dust control due to the risk of respirable silica exposure. Aluminium oxide is a synthetic abrasive known for its high hardness and angular particle morphology, making it widely used in applications requiring stronger cutting action and surface profiling. In industrial practice, abrasive selection depends on the substrate material, required surface cleanliness, desired surface profile, coating system, and allowable surface deformation. Other abrasives commonly used in industry include steel grit, steel shot, garnet, glass beads, silicon carbide, crushed slag, ceramic grit, and plastic media. The two media, silica sand and aluminium oxide, were sieved to confirm grit range and oven-dried before use to minimize agglomeration due to moisture. Fresh abrasive was used for each trial to avoid contamination and grit degradation.

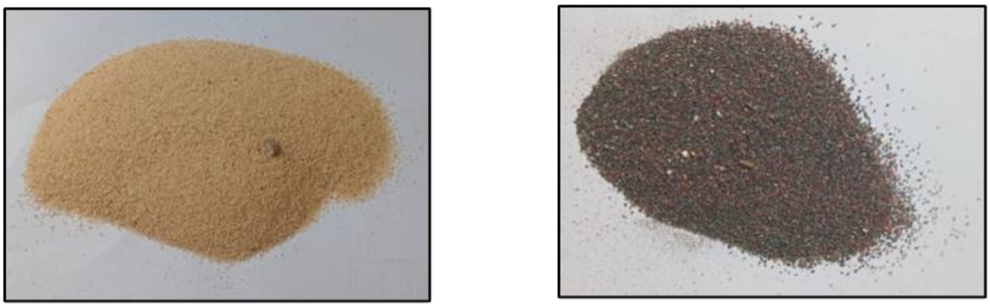

(a) (b)

Figure 2. Photographic representation of the two abrasive media **(a)** Silica, 60 mesh **(b)** Aluminium oxide, 60 Mesh.

2.2. Equipment and experimental setup

The sandblasting process, as illustrated in **Figure 3**, operates through a controlled flow of compressed air and abrasive particles directed toward the workpiece surface. The setup consists of a compressor, dryer, air regulator, blasting pot, nozzle, blasting chamber, and dust collector or blower. The process begins with high-pressure air from the compressor flowing into the sand tube. The compressed air then mixes with the abrasive sand, after which the air–sand mixture is directed toward the nozzle. Finally, the nozzle propels the high-pressure abrasive stream onto the surface of the workpiece. The sandblasting machine used in this study was locally and custom-built following a Capstone Design approach to ensure optimal performance[8], allowing modifications for precise control of air pressure, nozzle distance, and angle alignment. This flexible design ensured consistent abrasive flow and uniform surface coverage, improving experimental repeatability.

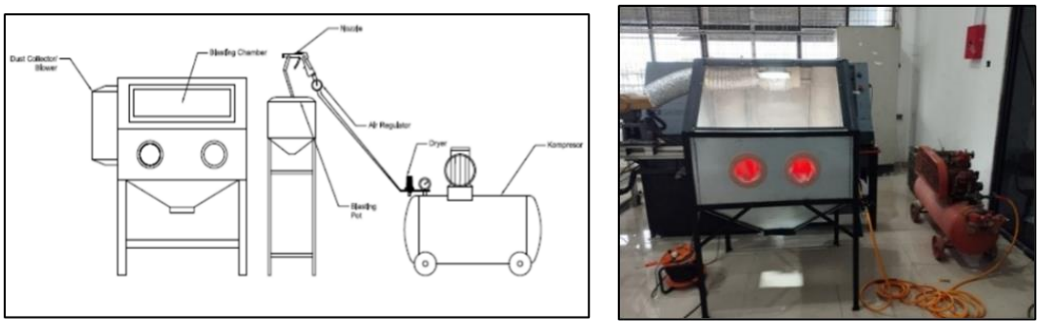

(a) (b)

Figure 3. (a) Schematic representation and **(b)** photographic view of the sandblasting setup used in this study.

2.3. Experimental variables and procedures

2.3.1. Experimental variables

The sandblasting process, as illustrated in **Figure 3**, operates through a controlled flow of compressed air and abrasive particles directed toward the workpiece surface.

The study involves the following variables:

1. Independent variables: abrasive media type, blasting pressure, and nozzle/impact angle.
2. Controlled variables: specimen material, grit/mesh size, nozzle distance, blasting procedure, and measurement method.
3. Dependent variables: Ra, Rp, Rz, mass loss, and surface morphology.

2.3.2. Experimental procedures

The experimental procedure was designed to systematically investigate the effect of abrasive type, air pressure, and impact angle on the surface roughness of ASTM A36 steel. All tests were conducted under controlled laboratory conditions to minimize environmental influence. The following steps describe the procedure in detail:

1. Specimen Preparation: ASTM A36 steel plates were cut into specimens measuring 100 mm × 50 mm × 3 mm using a handheld grinder, producing a total of eight samples. Each specimen was labeled with a unique identifier.
2. Surface Cleaning: The specimens were cleaned using alcohol applied evenly with a cloth or tissue, then air-dried to remove contaminants before testing.
3. Initial Roughness Measurement: Surface roughness was measured at three horizontal points (left, center, and right) on each specimen using a surface roughness tester, and the readings were recorded.
4. Sandblasting Process: Sandblasting was conducted using silica sand and aluminium oxide abrasives at air pressures of 5 bar and 7 bar, with impact angles of 45° and 90°. Each condition was applied alternately across the specimens to ensure consistent comparison.
5. Post-Blasting Cleaning: Residual abrasive particles and dust were removed using high-pressure air to prevent interference with subsequent measurements.
6. Final Roughness Measurement: After sandblasting, the surface roughness of each specimen was measured again using the same procedure as before.
7. Microscopic Analysis: Scanning Electron Microscopy (SEM) was performed on all specimens to examine surface morphology and compare microstructural differences between blasting conditions.

8. Data Analysis: The pre- and post-treatment roughness data were compared, and SEM observations were analyzed.

2.4. Surface characterization methods

Surface texture was quantified using a Mitutoyo SJ-310 surface roughness tester which can be seen in **Figure 4**. Prior to testing the instrument was calibrated with a certified roughness standard. For each specimen, measurements were taken at multiple, non-overlapping locations oriented both along and perpendicular to the blasting direction; three repeated traces per location were recorded and averaged to produce the reported value. Evaluation length and cutoff were chosen in accordance with ISO 4287/4288 recommendations, and the surface roughness tester settings (traverse speed and stylus radius) were set to the manufacturer's guidance to ensure reliable results.

Figure 4. Mitutoyo SJ-310 contact stylus profilometer employed for surface roughness measurement in accordance with ISO 4287/4288.

Scanning electron microscopy (SEM). Surface morphology was examined using SEM to visualize impact craters, cutting/peening marks, and any embedded abrasive particles. Specimens were cleaned with compressed air and an appropriate solvent, mounted to ensure electrical continuity, and imaged at 100×, 200×, and 600× to capture surface details at different observation scales. The 100× magnification provided a general overview of surface uniformity and crater distribution across the blasted area. The 200× magnification allowed for intermediate inspection of overlapping impacts, while the 600× magnification was used to examine fine-scale topographical features such as micro-grooves, sharp ridges, and embedded abrasive fragments. Secondary-electron imaging emphasized topographic contrast; if surface charging occurred, a thin conductive coating (Au/Pd, < 10 nm) was applied. Representative micrographs were correlated with roughness measurements to interpret how surface features contribute to the measured texture.

3. Results and discussion

3.1. Overview of experimental conditions

The sandblasting tests were carried out on eight specimens, with each condition defined by a specific combination of abrasive media type, blasting pressure, nozzle angle, mesh size, and stand-off distance. Environmental parameters, such as ambient temperature, were also recorded during each run to capture potential influences on the process. The detailed parameters for each specimen are summarized in **Table 2**.

Table 2. Parameters in sandblasting process.

Specimen	Abrasive Media	Pressure (bar)	Nozzle Angle (°)	Mesh	Distance (cm)	Temperature (°C)
A1	Silica	5	45	60	5	33.2
A2	Silica	5	90	60	5	33.4
A3	Silica	7	45	60	5	34.1
A4	Silica	7	90	60	5	34.7
B1	Al_2O_3	5	45	60	5	35.6
B2	Al_2O_3	5	90	60	5	36.2
B3	Al_2O_3	7	45	60	5	38.1
B4	Al_2O_3	7	90	60	5	38.6

Table 3 presents photographic records of the eight ASTM A36 steel specimens after sandblasting. Specimens A1–A4 were treated using silica sand, while specimens B1–B4 were treated using aluminium oxide. All images were captured using the same camera and lighting settings to enable direct visual comparison. These visual observations reveal differences in texture and uniformity between the two abrasive media, which are further quantified through surface roughness measurements and examined in greater detail via SEM imaging in Subsection 3.4.

Table 3. Photo documentation of the specimen after the sandblasting process.

Specimen	Documentation photo	Specimen	Documentation photo
A1	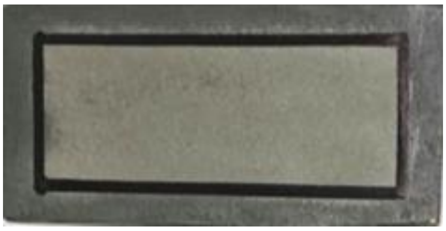	B1	
A2	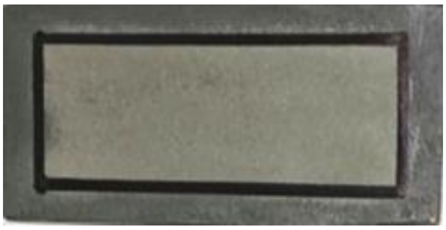	B2	
A3	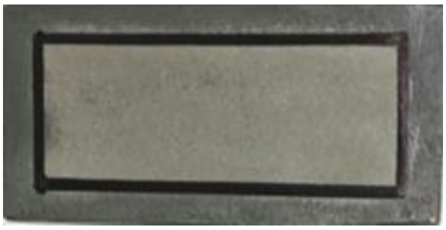	B3	
A4	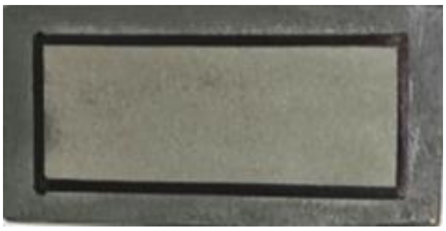	B4	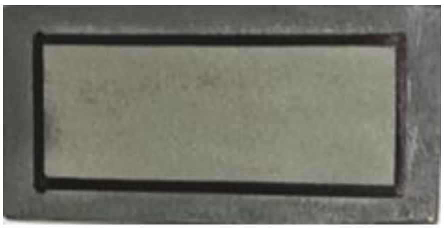

3.2. Surface roughness measurement results

3.2.1. Arithmetic average roughness (Ra) results

Ra is the arithmetic average of the absolute deviations of the surface profile from the mean line over a specified evaluation length. It provides a general representation of the overall surface roughness and is the most commonly used parameter for assessing surface texture. In this study, Ra measurements were taken for all specimens both before and after the sandblasting process. Each specimen was measured at three points, and the results are summarized in **Tables 4** and **5**.

Before sandblasting, the A-series specimens had average surface roughness (Ra) values ranging from 2.031 µm (A3) to 2.170 µm (A2). After sandblasting, these values increased significantly, with the lowest post-treatment value being 2.650 µm (A1) and the highest being 3.651 µm (A4). The increases in Ra for the silica sand group ranged from +0.549 µm (A1) to +1.506 µm (A4). This demonstrates that silica sand blasting effectively increased surface roughness, although the magnitude of increase varied among specimens. The variation may be due to differences in the surface condition or slight inconsistencies in the nozzle angle and exposure time.

Before sandblasting, the B-series specimens showed average Ra values from 1.789 µm (B3) to 1.891 µm (B2), which were generally smoother than the A-series specimens prior to treatment. After sandblasting, these values rose to between 2.593 µm (B1) and 3.819 µm (B4). The increase for aluminium oxide blasting ranged from +0.787 µm (B1) to +2.021 µm (B3). The higher increases, especially in specimens B3 and B4, indicate that aluminium oxide—being harder and sharper than silica sand—produced deeper and more aggressive surface texturing.

Table 4. Ra data before sandblasting.

Specimen	Ra (Average)
A1	2.101
A2	2.170
A3	2.031
A4	2.145
B1	1.806
B2	1.891
B3	1.789
B4	1.832

Table 5. Ra data after sandblasting.

Specimen	Ra (Average)
A1	2.650
A2	2.804
A3	3.523
A4	3.651
B1	2.593
B2	2.999
B3	3.810
B4	3.819

From **Table 2** on angle variations, it can be seen that silica abrasive particles on specimens A1 and A3, as well as aluminium oxide on specimens B1 and B3, do not produce sufficient energy to form a pronounced roughness profile. This is due to the nozzle position not being perpendicular to the specimen surface, causing the abrasive particles to strike at an angle and reducing their cutting and deforming effectiveness.

To evaluate the effect of nozzle angle, specimens should be compared at the same blasting pressure. At 5 bar, the 90° specimens A2 and B2 showed higher Ra values than their 45° counterparts A1 and B1. Similarly, at 7 bar, A4 and B4 showed higher Ra values than A3 and B3, respectively. This indicates that a perpendicular nozzle angle enhances the normal impact component of abrasive particles, resulting in greater surface deformation and higher roughness. The variation in Ra values is presented in **Figure 5**, which clearly compares the surface roughness before and after sandblasting.

The interaction between abrasive type, pressure, and impact angle reveals a synergistic effect on the resulting roughness. Higher pressure and perpendicular angles amplify the cutting energy transferred to the steel surface, while the abrasive hardness determines the extent of plastic deformation. Aluminium oxide, being denser and sharper, maintains its shape at higher pressures, causing deeper penetration and more consistent crater formation compared to silica sand. In contrast, silica tends to fracture upon impact, dispersing its kinetic energy and producing smoother textures. This behavior indicates that while angle and pressure dictate the overall kinetic contribution, abrasive type governs the micro-mechanical interaction at the material surface, collectively shaping the final roughness pattern.

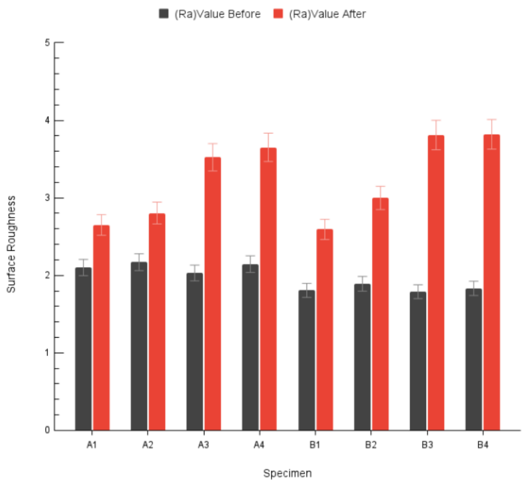

Figure 5. Comparison of average Ra values before and after sandblasting.

3.2.2. Maximum profile peak height (Rp) results

Rp is the height of the highest peak above the mean line within the sampling length. It reflects the most prominent surface protrusion and is important when peak height can influence performance, such as in sealing or wear applications.

Table 6. Rp data before sandblasting.

Specimen	Rp (Average)
A1	6.976
A2	6.616
A3	6.415
A4	7.267
B1	5.668
B2	6.133
B3	5.016
B4	4.823

Based on the data presented in **Tables 6** and **7**, the Rp values prior to sandblasting for the silica sand group (A-series) ranged from 6.415 µm (A3) to 7.267 µm (A4), while the aluminium oxide group (B-series) ranged from 4.823 µm (B4) to 6.133 µm (B2). These findings indicate that, before treatment, the silica sand specimens generally exhibited greater peak heights compared to the aluminium oxide specimens.

After sandblasting, Rp values generally increased, except for specimen A1, demonstrating that the process generated more pronounced surface peaks. In the silica sand group, the highest post-treatment Rp was recorded in specimen A4 (10.140 µm), with the lowest in A1 (6.841 µm). For the aluminium oxide group, the highest value was observed in B2 (7.767 µm) and the lowest in B3 (6.841 µm). These results also shown in **Figure 6** confirm that sandblasting effectively enhances peak height, with silica sand generally producing larger increases than aluminium oxide under the same conditions.

Table 7. Rp data after sandblasting.

Specimen	Rp (Average)
A1	6.841
A2	7.765
A3	10.008
A4	10.140
B1	7.394
B2	7.767
B3	6.841
B4	7.765

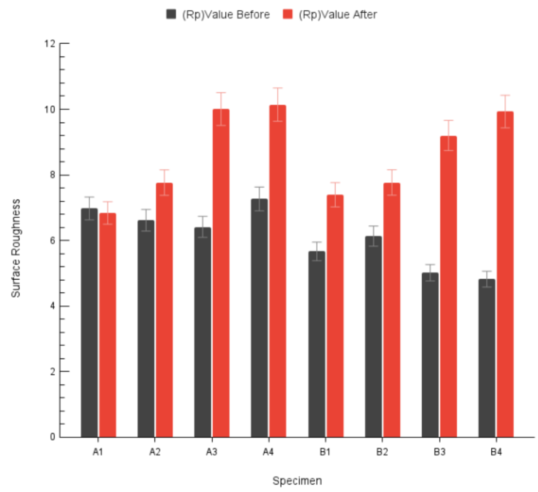

Figure 6. Comparison of average Rp values before and after sandblasting.

3.2.3. Average maximum height of the profile (Rz) results

Rz represents the average vertical distance between the highest peak and the lowest valley across several sampling lengths (typically five).

Table 8. Rz data before sandblasting.

Specimen	Rz (Average)
A1	12.350
A2	12.208
A3	11.738
A4	12.797
B1	11.714
B2	10.669
B3	9.298
B4	9.717

This parameter reflects the total peak-to-valley height, providing a comprehensive indication of surface topography by accounting for both protrusions and depressions in the profile.

Table 9. Rz data after sandblasting.

Specimen	Rz (Average)
A1	15.427
A2	16.872
A3	20.570
A4	22.674
B1	16.447
B2	17.525
B3	20.003
B4	22.689

From the results shown in **Tables 8** and **9**, it can be observed that before sandblasting, the silica sand group (A-series) exhibited Rz values between 11.738 µm (A3) and 12.797 µm (A4). In contrast, the aluminium oxide group (B-series) recorded lower initial values, ranging from 9.298 µm (B3) to 11.714 µm (B1). This indicates that the untreated surfaces in the silica sand group generally had greater peak-to-valley heights compared to those in the aluminium oxide group.

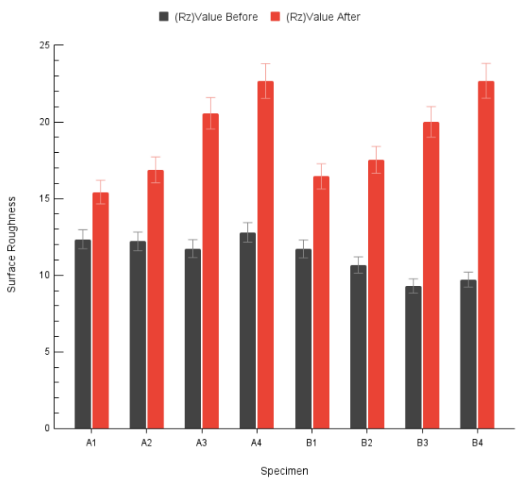

Figure 7. Comparison of average Rz values before and after sandblasting.

After sandblasting, a marked increase in Rz values was observed for all specimens, signifying that the process enhanced the overall surface relief by both raising peak heights and deepening valleys. In the silica sand group, the highest Rz value after treatment was found in specimen A4 (22.674 µm), while the lowest was in A1 (15.427 µm). Meanwhile, in the aluminium oxide group, post-treatment values ranged from 16.447 µm (B1) to 22.689 µm (B4). These findings, also illustrated in **Figure 7**, confirm that sandblasting produced a more pronounced and textured surface profile across all samples.

These trends from **Figures 5-7** are consistent with the interaction behavior discussed in the Ra analysis, where higher pressure and perpendicular angles enhanced kinetic energy transfer, especially when combined with harder abrasives. The observed increase in surface roughness with higher pressure and perpendicular angles aligns with findings by Putri et al.[5], Sugiantoro et al.[9], Bechikh et al.[10], and Adiansyah et al.[11] who reported similar trends in carbon and structural steels. Aldio et al.[12] reported that finer silica sand and repeated blasting cycles significantly increase roughness and cleanliness of SS400 steel surfaces under 7 bar pressure, supporting the role of impact energy and abrasive size on surface profiling. These consistent results reinforce that abrasive hardness and impact direction collectively determine surface roughness characteristics and coating adhesion performance[13].

3.3. Results of weight loss analysis

The specimens were weighed using a digital scale with an accuracy of 0.1 g both before and after the sandblasting process. The recorded measurements are presented in **Table 10**.

Table 10. Mass data before and after sandblasting.

Specimen	Start Mass (g)	End Mass (g)	Mass loss
A1	114.8	114.5	0.3
A2	109.1	108.9	0.2
A3	109.2	109.1	0.1
A4	115.5	115.3	0.2
B1	116.6	116.3	0.3
B2	110.8	110.7	0.1
B3	111.3	111.2	0.1
B4	112.5	112.3	0.2

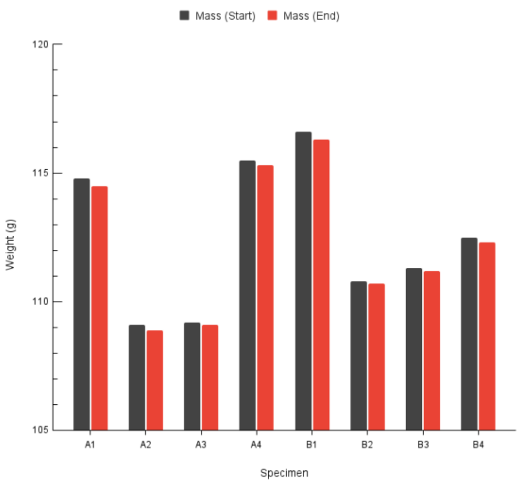

Figure 8. Comparison of specimen mass before and after sandblasting.

Based on **Table 10** and **Figure 8**, the weight loss of the specimens after the sandblasting process was relatively minimal, ranging from 0.1 to 0.3 grams. This limited reduction is attributed to the absence of repeated blasting cycles during the process. The percentage decrease in weight for each specimen is as follows: A1 – 0.26%, A2 – 0.18%, A3 – 0.09%, A4 – 0.17%, B1 – 0.25%, B2 – 0.09%, B3 – 0.08%, and B4 – 0.17%.

3.4. Scanning Electron Microscope Results

SEM testing was conducted to observe the morphological characteristics of the ASTM A36 steel surface following the sandblasting process. **Table 11** presents SEM micrographs of ASTM A36 steel surfaces after sandblasting with silica and aluminium oxide abrasives at magnifications of 100×, 200×, and 600×. Each image was captured under identical conditions to ensure accurate visual comparison. For both abrasive media, the overall surface texture becomes progressively clearer and more detailed with increasing magnification.

From visual inspection, specimens treated with aluminium oxide exhibit a surface that is noticeably more wavy and irregular compared to those blasted with silica. At lower magnifications (100× and 200×), silica-treated specimens display a more uniform texture with smoother, evenly distributed wave patterns, whereas aluminium oxide produces a rougher and more heterogeneous surface.

At higher magnification (600×), the aluminium oxide-treated specimens reveal deeper indentations and more pronounced surface perforations than those treated with silica. This indicates that aluminium oxide is more effective in producing higher surface roughness, which can enhance cleaning efficiency and surface preparation, compared to silica abrasive media.

Table 11. SEM micrographs of ASTM A36 steel surfaces after sandblasting with silica and aluminium oxide abrasives at various magnifications (100×, 200×, 600×).

Silica abrasive	Aluminium oxide abrasive	Magnification
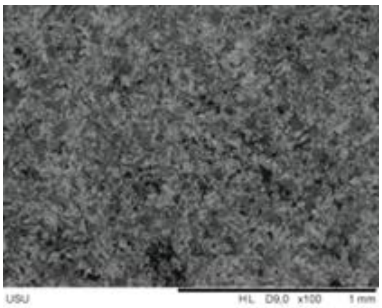	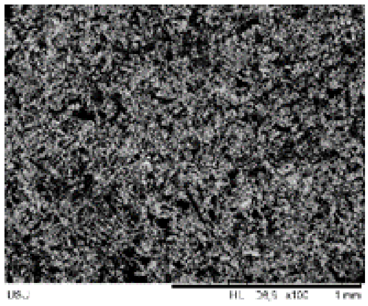	100×
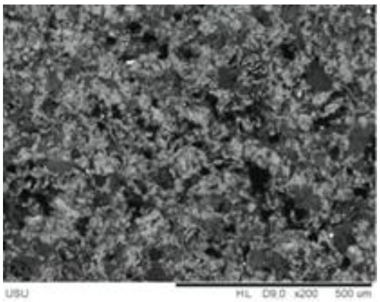	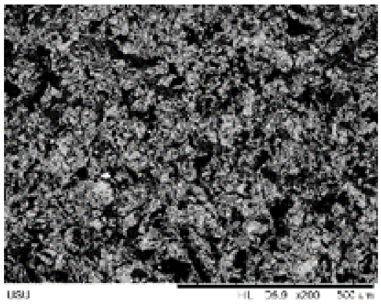	200×
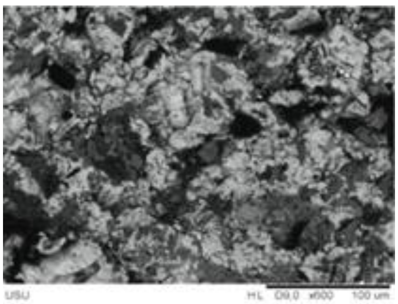	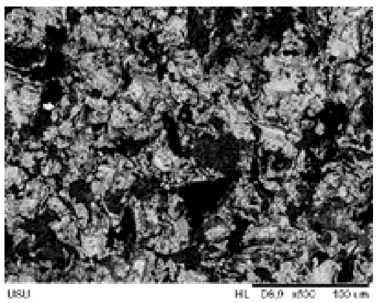	600×

From a practical standpoint, these findings have significant implications for industrial surface preparation and coating applications. The enhanced roughness produced by aluminium oxide at higher pressures and perpendicular angles can improve mechanical interlocking and coating adhesion in processes such as painting, electroplating, and thermal spraying. The SEM images suggest a more irregular surface morphology after aluminium oxide blasting. Although the SEM images provide qualitative evidence of surface deformation, impact craters, grooves, and abrasive-induced irregularities, they do not fully quantify the three-dimensional surface topography of the sandblasted surface. Therefore, future work should include 3D surface profilometry, optical profilometry, or confocal laser scanning microscopy to evaluate surface height distribution, peak density, valley depth, and surface uniformity. This additional analysis would provide a stronger correlation between sandblasting parameters, roughness profile, and coating adhesion performance. This optimization is particularly valuable in the automotive, shipbuilding, and construction industries, where ASTM A36 steel is widely used and consistent surface preparation is critical for corrosion resistance and fatigue performance. Moreover, understanding the relationship between abrasive selection and blasting parameters enables industries to balance cost efficiency and surface quality—silica may be preferable for preliminary cleaning, while aluminium oxide suits applications requiring strong coating adhesion and durability.

3.5. Practical Assessment of Sandblasted Surface Roughness for Coating Adhesion

The surface roughness results obtained in this study provide an important basis for evaluating the suitability of the sandblasted ASTM A36 steel surface for coating applications. In coating systems, surface roughness is not only a visual or dimensional parameter, but also an important factor controlling mechanical interlocking between the coating layer and the steel substrate. A properly roughened surface can increase the effective contact area and provide anchor points for the coating, thereby improving adhesion strength. This relationship is consistent with Wijaya et al. (2024), who reported that abrasive blast cleaning of ASTM A36 steel produced the highest surface roughness and the highest coating adhesion strength compared with other surface preparation methods[14]. A rough interfacial profile can improve coating adhesion by increasing mechanical interlocking, but coating durability also depends on the integrity of the coating-substrate interface[15]. Previous work on steel painting systems has shown that surface preparation strongly affects surface morphology, pull-off adhesion, and protective coating performance[16]. However, excessive or uncontrolled roughness may also be detrimental because very sharp peaks, deep valleys, and non-uniform profiles can lead to incomplete coating wetting, trapped air, local stress concentration, and early coating failure. Surface roughness and surface chemistry should be considered together because both can influence initial adhesion and degradation at the coating–substrate interface[17].

Based on the Ra results, all sandblasting conditions increased the surface roughness of ASTM A36 steel compared with the initial condition. For the silica abrasive specimens, the average Ra increased from approximately 2.031-2.170 µm before blasting to 2.650-3.651 µm after blasting. For the aluminium oxide specimens, the average Ra increased from approximately 1.789-1.891 µm before blasting to 2.593-3.819 µm after blasting. The highest Ra value was obtained for specimen B4, treated with aluminium oxide at 7 bar and 90°, with an average Ra of 3.819 µm, while the highest silica-treated specimen was A4, treated at 7 bar and 90°, with an average Ra of 3.651 µm. These results indicate that higher pressure and a perpendicular impact angle are more effective in generating a rougher steel surface, which is generally beneficial for coating adhesion because it promotes stronger mechanical anchoring.

The effect of nozzle angle is particularly important when the surface is assessed for coating adhesion. At 45°, the abrasive particles strike the steel surface with a lower normal impact component, so part of the particle energy is converted into sliding or tangential motion. This condition can still clean and roughen the surface, but it tends to produce a less pronounced surface profile. In contrast, at 90°, the abrasive particles impact the surface more directly, allowing greater energy transfer into the substrate. This produces deeper indentations, higher profile development, and greater roughness. This trend can be seen from the Ra values, where both silica and aluminium oxide abrasives produced higher roughness at 90° than at 45° under comparable pressure conditions. Therefore, the 90° angle is more suitable when the main objective is to increase surface profile for coating anchorage.

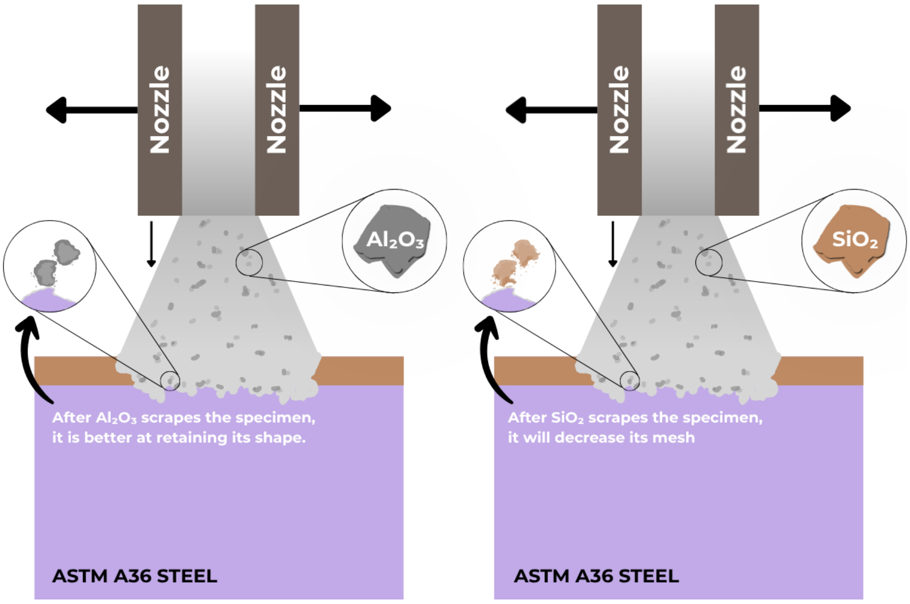

Figure 9. Schematic illustration of the different abrasive-surface interaction mechanisms during sandblasting of ASTM A36 steel using aluminium oxide and silica abrasives.

The Rp and Rz results provide additional information beyond Ra. While Ra describes the average roughness, Rp represents the highest peak above the mean line, and Rz represents the average peak-to-valley height. These parameters are important for coating adhesion because coating performance depends not only on the average surface roughness but also on the shape and depth of the surface profile. Pull-off adhesion strength is influenced not only by roughness magnitude, but also by the morphology of the surface profile, including whether the profile is sharp, angular, or rounded[18]. Recent studies also emphasize that surface topography should be considered together with roughness parameters because coating performance depends on surface height distribution, surface irregularity, and coating–substrate interaction[19]. After sandblasting, the Rz values increased substantially for both abrasive types, reaching 22.674 µm for silica at 7 bar and 90° and 22.689 µm for aluminium oxide at 7 bar and 90°. This shows that both abrasives were able to form pronounced peak-to-valley profiles under the most severe blasting condition. A higher Rz value may improve coating anchorage by providing deeper valleys for the coating to penetrate, but excessive peak-to-valley depth may also require sufficient coating thickness to fully cover the surface profile. If the coating is too thin, high peaks may remain insufficiently covered, increasing the risk of coating defects or premature corrosion initiation.

The comparison between silica and aluminium oxide shown in **Figure 9**, suggests that aluminium oxide is slightly more effective in increasing Ra under the highest pressure and perpendicular angle condition. This can be attributed to the higher hardness and angular morphology of aluminium oxide particles, which allows stronger cutting and indentation of the steel surface. Meanwhile, silica abrasive also produced significant surface profiling, especially at 7 bar and 90°, as indicated by its high Rz and Rp values. This implies that silica can still be suitable for moderate surface preparation, while aluminium oxide is more appropriate when a stronger surface profile is required. However, the selection of abrasive material should consider not only roughness improvement but also cost, abrasive durability, possible particle embedment, health and safety issues, and the required coating specification.

For practical coating applications, the results indicate that the 7 bar and 90° condition provides the most favorable surface profile among the tested parameters because it produced the highest Ra and Rz values. This condition may be recommended when the target is to improve coating adhesion through mechanical interlocking. Nevertheless, the surface should not be evaluated using Ra alone. A high Ra value must be supported by a balanced surface profile, where the peaks are not too sharp and the valleys are accessible for coating penetration. Therefore, the combined evaluation of Ra, Rp, and Rz is more useful than relying only on average roughness. In this study, the high Rz values at 7 bar and 90° suggest strong profile formation, but further adhesion testing, such as pull-off adhesion testing, cross-cut testing, or scratch testing, is required to directly confirm the improvement in coating adhesion.

The SEM observations support the roughness measurement results by showing more irregular surface morphology after blasting, especially for aluminium oxide-treated surfaces. However, SEM images should be interpreted as qualitative evidence only. They can help visualize surface deformation, craters, and possible abrasive residues, but they cannot fully quantify the three-dimensional surface topography. Therefore, future work should include 3D surface profilometry and surface composition analysis such as EDS/EDX. Three-dimensional morphology would provide clearer information about peak distribution, valley depth, and surface uniformity, while EDS/EDX would confirm whether silica or aluminium oxide particles remain embedded on the ASTM A36 steel surface after blasting. These additional analyses would strengthen the connection between sandblasting parameters, surface topography, and coating adhesion performance.

Overall, the roughness data show that sandblasting with higher pressure and perpendicular impact angle improves the surface profile of ASTM A36 steel, which is beneficial for coating adhesion through increased surface area and mechanical interlocking. Among the tested conditions, aluminium oxide at 7 bar and 90° produced the highest Ra value, while both silica and aluminium oxide at 7 bar and 90° produced high Rz values. Therefore, these conditions are the most promising for coating preparation. However, the optimum blasting condition should be selected according to the intended coating system, because excessive roughness, sharp peaks, and possible abrasive embedment may reduce coating quality if not properly controlled. Future studies should directly correlate the measured roughness values with coating adhesion strength to determine the most effective surface preparation condition for ASTM A36 steel.

4. Conclusion

Based on the surface morphology observed through SEM analysis and the measured roughness values, it is evident that both abrasive type and nozzle angle significantly influence the resulting surface texture of ASTM A36 steel. The following conclusions can be drawn from the experimental results:

1. Surface roughness increased with higher blasting pressure and a more perpendicular nozzle angle. The highest roughness (3.819 μm) was achieved using aluminium oxide at 7 bar and 90°, while the lowest (2.593 μm) occurred at 5 bar and 45°.
2. A 90° nozzle angle provides optimal impact, as the abrasive particles strike the ASTM A36 steel surface perpendicularly, maximizing material removal and surface modification.
3. Aluminium oxide produced greater roughness than silica under the highest pressure and perpendicular nozzle angle, likely due to its higher hardness and angular morphology. However, abrasive selection should also consider cost, safety, durability, and reusability, which were not directly evaluated in this study.

This study contributes valuable insight into optimizing sandblasting parameters for industrial surface preparation, particularly for ASTM A36 steel. The results can guide the selection of abrasive materials and process settings to enhance coating adhesion and durability. Future research should expand to include long-term coating performance, energy efficiency, and cost analysis under various industrial conditions. In addition, future work should directly correlate the measured roughness parameters with coating adhesion strength through pull-off, cross-cut, or scratch testing. Further 3D surface profilometry and surface composition analysis, such as EDS/EDX, are also recommended to evaluate peak distribution, valley depth, surface uniformity, and possible abrasive residue embedment on the ASTM A36 steel surface.

Author contributions

Conceptualization, Riky Stepanus Situmorang and Novin Haritsyah; Methodology, Riky Stepanus Situmorang and Novin Haritsyah; Investigation, Novin Haritsyah and James Haryanto; Formal analysis, Novin Haritsyah and James Haryanto; Data curation, Novin Haritsyah and James Haryanto; Writing—original draft preparation, Novin Haritsyah and James Haryanto; Writing—review and editing, James Haryanto; Visualization, Novin Haritsyah; Supervision, Hendrik Voice Sihombing and Riky Stepanus Situmorang; Project administration, Hendrik Voice Sihombing and Riky Stepanus Situmorang. All authors have read and agreed to the published version of the manuscript.

Acknowledgments

The work was supported by the Universitas Sumatera Utara with Grant number: 9451/UN5.2.1.4/SK/KPM/2024.

Conflict of interest

The authors declare no conflict of interest.

References

1. Baktiono, R. B., Pengaruh sudut dan jarak penembakan pada proses sandblasting terhadap kekasaran permukaan baja SS400, Undergraduate Thesis, Universitas Brawijaya, (2019). Available at: https://repository.ub.ac.id/id/eprint/178394
2. Saputra, B., Pengaruh pengulangan penyemprotan dan ukuran pasir silika pada proses sandblasting terhadap kekasaran permukaan baja SS400, Undergraduate Thesis, Universitas Islam Riau, (2020). Available at: https://repository.uir.ac.id/id/eprint/13235
3. A. Rudawska, I. Danczak, M. Müller, P. Valasek, The effect of sandblasting on surface properties for adhesion. Int. J. Adhes. Adhes. 70, 176–190 (2016). https://doi.org/10.1016/j.ijadhadh.2016.06.010
4. M. Iqbal Mukhsen, Pengaruh jenis abrasif pada proses shotpeening terhadap kekasaran permukaan dan kekerasan baja tahan karat. Prosiding Seminar Nasional Penelitian & Pengabdian Kepada Masyarakat 2019, 137–143 (2019). ISBN 978-602-60766-7-0.
5. F. Putri, I. HB, E. Pratama, Analisa pengaruh tekanan kompresor dan sudut penyemprotan pada proses sandblasting terhadap uji kekasaran pada baja ST 50. J. Austenit 11(1), 21–24 (2019). ISSN 2085-1286 / E-ISSN 2622-7649.
6. B. Śmielak, L. Klimek, K. Krześniak, Effect of sandblasting parameters and the type and hardness of the material on the number of embedded Al_2O_3 grains. Mater. 16, 4783 (2023). https://doi.org/10.3390/ma16134783
7. W. Pamungkas, Y. Amalia, R.Z. Miratahti, Pengaruh jarak nozzle sandblasting baja SS400 terhadap ketebalan coating dan laju korosi. J. Energi Manuf. 15(2), 116–121 (2022). https://doi.org/10.24843/JEM.2022.v15.i02.p08
8. R.S. Situmorang, M. Prasetya, J. Haryanto, M. Sabri, Design and construction of sandblasting tools for metal surface cleaner. J. Dinamis 13(1), 53–63 (2025). https://doi.org/10.32734/dinamis.v13i1.21854
9. Sugiantoro, D. Dwilaksana, G. Jatisukamto, Analisis kekasaran permukaan proses sandblasting dengan variasi tekanan, waktu dan sudut menggunakan metode Taguchi. J. Proteksion 2(1), 27–30 (2017). ISSN 2528-6382 / E-ISSN 2541-3562
10. A. Bechikh, O. Klinkova, Y. Maalej, I. Tawfiq, R. Nasri, Sandblasting parameter variation effect on galvanized steel surface chemical composition, roughness and free energy. Int. J. Adhes. Adhes. 102, 102653 (2020). https://doi.org/10.1016/j.ijadhadh.2020.102653
11. M. Adiansyah, Kasir, M. W. Junaidi, Pengaruh tekanan udara sandblasting terhadap kekasaran permukaan pada baja karbon ST 60. Diploma Thesis, Department of Mechanical Engineering, Politeknik Harapan Bersama, Tegal (2021). Available at: https://eprints.poltektegal.ac.id/789/
12. R.Z. Aldio, D. Dedikarni, B. Saputra, I. Anwar, M.S. Masdar, Effect of spraying and mesh size on surface roughness of SS400 steel sandblasting process. J. Renew. Energy Mech. 4(2), 63–75 (2021). https://doi.org/10.25299/rem.2021.vol4(02).7500
13. F. W. Hapsari, H. Pratikno, W. L. Dhanista, Analisis pengaruh variasi material abrasif dan ketebalan polyurethane coating pada baja ASTM A36 terhadap laju korosi di lingkungan air laut. J. Tek. Mesin Mater. Energi 4(3), 113–120 (2020). https://doi.org/10.12962/j2580-0914.v4i3.9953

14. Wijaya, I., Aqila, D., Riastuti, R., & Ramadhani, R. T. (2024). Analysis the effect of different surface preparation methods on corrosion resistance and adhesion strength of ASTM A36 steel substrate with surface tolerant epoxy paint as coating material. Journal of Engineering and Scientific Research, 6(1), 52–60. https://doi.org/10.23960/jesr.v6i1.152
15. Croll, S. G. (2020). Surface roughness profile and its effect on coating adhesion and corrosion protection: A review. Progress in Organic Coatings, 148, 105847. https://doi.org/10.1016/j.porgcoat.2020.105847
16. Jamali, S. S., Mills, D. J., & Paprocka, K. (2014). Steel surface preparation prior to painting and its impact on protective performance of organic coating on steel. Progress in Organic Coatings, 77(12), 2091–2099. https://doi.org/10.1016/j.porgcoat.2014.04.018
17. Van Dam, J. P. B., Abrahami, S. T., Yilmaz, A., Gonzalez-Garcia, Y., Terryn, H., & Mol, J. M. C. (2020). Effect of surface roughness and chemistry on the adhesion and durability of a steel–epoxy adhesive interface. International Journal of Adhesion and Adhesives. https://doi.org/10.1016/j.ijadhadh.2019.102450
18. Kambhampati, S., Cao, Q., Ghodkay, V., Farhat, H., & Pojtanabuntoeng, T. (2023). A study on the effect of surface profile on pull-off adhesion strength value of organic coatings. AMPP Annual Conference + Expo, AMPP-2023-19225.
19. Sługocka, M., et al. (2024). Study of the impact of surface topography on selected properties of coatings. Coatings, 14(8), 944. https://doi.org/10.3390/coatings14080944